Kinetics of DNA Binding to Electrically Conducting Polypyrrole Films

Daniel S. Minehan,† Kenneth A. Marx,* and Sukant K. Tripathy

Department of Chemistry and Center for Advanced Materials, University of Massachusetts, Lowell, One University Avenue, Lowell, Massachusetts 01854

Received March 16, 1992; Revised Manuscript Received October 25, 1993®

ABSTRACT: We investigated the kinetics of ^{32}P end labeled DNA binding from solution to electrochemically prepared polypyrrole (PPy) thick films. These data were found to fit a simple diffusion-limited binding model with low phenomenological activation energy (5 kcal/mol), consistent with diffusion-limited binding kinetics. These data suggest that the DNA binds to PPy without significant alteration of its structure. The binding of double-helical DNA to PPy was found to be dependent upon the presence of the electrooxidized positively charged surface functional groups on PPy. DNA adsorption kinetics are only moderately affected by changes in ionic strength and pH in the 5–9 range. A twofold increase in binding rate is observed for single-stranded DNA compared to the double-stranded DNA binding level. DNA desorption and competitor-driven desorption studies were performed to characterize the binding state and release of DNA from the polypyrrole substrates. These data suggested that a significant fraction of the DNA was reversibly bound, consistent with the low measured activation energy.

Introduction

The electrochemically oxidized form of polypyrrole, PPy, is electrically conducting in the range 10^{-3}–10^{3} $\Omega \cdot cm^{-1}$, depending on synthesis conditions.[1-5] Electrical conduction in PPy is the result of electron movement within delocalized π-band orbitals and topological positive charge defects known as polarons and bipolarons.[6-8] The positive charge defects are polarized and counterbalanced by oppositely charged dopant molecules that are incorporated during PPy synthesis.[9] There are three or four monomer repeat units along the polymer backbone for every dopant molecule[1,9] at high levels of doping. PPy is an attractive conducting polymer for research purposes, since it can be directly prepared as a flexible free-standing film[5] that maintains its conductivity for several months.[3,5]

There have been relatively few reports on the interaction of PPy or any other conducting polymer with biological macromolecules. Small molecules such as ferrocyanide and glutamate have been shown to be electrochemically released from PPy electrodes.[10] Other small-biomolecule interactions studied have included the binding and release of the neurotransmitter dopamine[11] and the doping of PPy with ATP.[12] An early study involving biological macromolecules was the incorporation of the enzyme glucose oxidase into PPy films.[13] These investigators were the first to demonstrate that incorporated glucose oxidase provided a biosensor for the rapid detection of glucose, remaining active for weeks. More recently, various proteins have been shown to bind to chemically prepared PPy,[14] and a study involving the interaction of polycatonic histone proteins with poly(styrenesulfonate)-doped PPy films has been reported.[15] This latter report is relevant to the present study since histones are among those proteins known to interact with DNA in cells. The present study represents the first report of a direct interaction of a conducting polymer with a polynucleotide.

Phenomenologically, DNA has been shown to bind to solid surfaces through noncovalent interactions. DNA can be purified from other components through preferential binding to solid-phase chromatographic materials such as nitrocellulose, hydroxyapatite, methylated albumin on Keiselguhr (MAK), and others.[16-20] However, quantitative, mechanistic oriented studies of noncovalent interactions are rarely found in the literature. Of great importance in research and biotechnological applications, the widely used nitrocellulose binding of denatured DNA in the Southern transfer/hybridization procedure and the noncovalent binding to nitrocellulose of DNA–protein complexes are little understood mechanistically.

In the case of DNA binding to hydroxyapatite, careful deoxyribonuclease digestion studies of DNA bound to the charged surface revealed a periodic cleavage pattern suggesting an undistorted double-helical structure.[21] Double-stranded DNA adsorption onto sand (SiO_2: a negatively charged polyelectrolyte) has also been described.[19]

The electrically conducting PPy polymer provides a unique surface for DNA binding in that its delocalized electronic structure allows positively charged groups mobility along the chain axis. This surface charge mobility leads us to speculate that DNA as a polyelectrolyte possessing a fixed negative charge distribution would bind very strongly since the surface positive charge could redistribute to maximize a favorable energetic interaction. The rationale for strong DNA binding to the PPy surface is also based upon the following two facts. PPy can interchange its negatively charged dopant molecules easily with other negatively charged species, including biomolecules.[12] Also, hydrogen bonding to phosphate oxygens in the DNA backbone can enhance binding to DNA, and PPy could provide such hydrogen bonds through its pyrrole ring nitrogen atom. Since previous studies have shown that glucose oxidase was able to remain enzymatically active entrapped in PPy films,[13] it is reasonable to suggest that a conformationally less sensitive biomolecule such as DNA should not be significantly altered on binding to the PPy surface.

In the present report we study ^{32}P radiolabeled DNA binding kinetics onto solid PPy substrates. The data follow a diffusion-limited kinetic binding model with low activation energy. Adsorption of certain proteins onto two-dimensional surfaces has previously been shown to follow a similar diffusion-limited binding model.[22-24] We also report the effects of buffer concentration and type, pH, and secondary structural state of the DNA (single strand

* To whom correspondence should be addressed.
† Current address: American Cast Iron Pipe Co., P.O. Box 2727, Birmingham, AL 35202-2727.
® Abstract published in *Advance ACS Abstracts,* January 1, 1994.

0024-9297/94/2227-0777$04.50/0

or double helix). The reversibility of double-helical DNA adsorption was demonstrated through desorption kinetics and competition studies with various polyelectrolytes.

Experimental Section

Electrochemical Polymerization. The electrochemical polymerizations were performed in the absence of mechanical agitation in a two-compartment cell designed with a graphite rod cathode, an anode compartment that held a smooth Pt plate (front side area of 32.5 cm^2), and a saturated calomel electrode (SCE) as the reference electrode. The power supply was a Model 231 Princeton Applied Research potentiostat–galvanostat.

Typically, a reaction vessel contained 200 mL of a 0.2 M solution of distilled pyrrole (99%, Aldrich Chemical Co., Inc.) holding 0.2 M tetraethylammonium *p*-toluenesulfonate (Aldrich) electrolyte in acetonitrile solvent (Fisher Scientific, Optima grade) mixed with distilled water to form a 2% solution by weight. Unless otherwise noted, chemicals were reagent grade. Pyrrole was distilled to a colorless purified form within 30 min prior to electropolymerization.

The current density was held constant at 1.0 mA/cm^2, which stabilized at a voltage of ca. 0.75 V vs SCE. After 5 h of reaction time a film of 50 μm had grown. The film was first rinsed, then soaked for 1 h in pure acetonitrile, and then peeled off with a razor blade and tweezers. The free-standing film was then soaked in 50 mL of pure acetonitrile for ca. 24 h. Poly(pyrrole–*p*-toluenesulfonate) (PPy/p-TS) films grown in a similar manner have a conductivity in the range 1–100 $\Omega^{-1}\cdot cm^{-1}$.[1,5]

Before samples were used in DNA binding studies, they were allowed to dry on standing in air, cut into 0.28-cm^2 circular polypyrrole disks, placed on weighing paper, and stored in polystyrene Petri dishes in the dark.

Radiolabeling of DNA. Enzymatic cleavage of the double-stranded replicative form $\phi X174$ DNA by *Hha*I produces 18 fragments of the following sizes: 1553, 640, 614, 532, 305, 300, 269, 201, 192, 145, 143, 123, 104, 101, 93, 84, 54, and 35 bp. The average fragment length is 299 bp, or 2×10^5 g/mol. The ^{32}P end labeling of 1 μg of *Hha*I-digested $\phi X174$ DNA was performed using a 3′ end labeling kit (New England Nuclear). The DNA was labeled at the 3′-hydroxyl ends with $\alpha^{32}P$-labeled cordecypin 5′-triphosphate catalyzed by terminal deoxynucleotidyl transferase at an incubation temperature of 37 °C, followed by ethanol precipitation. In practice, the specific activity per reaction ranged from 2×10^3 to 5×10^4 dpm/pmol. This was due primarily to storage time dependent loss of the high-energy phosphate bond in the radiolabeled precursor. Care had been taken to precipitate and centrifuge the DNA for 15 min rather than the suggested 5 min. Magnesium acetate (1–3 mM) was used instead of carrier transfer RNA to precipitate the DNA after incubation as RNA may severely alter the observable DNA binding in the experiments. The radiolabeled DNA for each labeling reaction was dissolved in 500 μL of a TE buffer: 1 mM EDTA and 10 mM Tris, at pH 8. The radiolabeled DNA was stored at 4 °C in a silanated polypropylene Eppendorf centrifuge tube to prevent loss due to nonspecific DNA adsorption. The storage time prior to the experiment varied from 1 to 14 days.

DNA–Polypyrrole Binding Kinetics. Sample droplets containing 0.2 μg/mL of ^{32}P-labeled DNA in 1X TE buffer were placed in droplet form on a polypropylene surface. The droplet was further placed within a covered Petri dish such that a TE buffer pool surrounded the polypropylene in order to prevent droplet evaporation. Droplets retained a constant volume for several days in this condition.

The disk shaped PPy substrate, lifted with electron microscopy tweezers, was then placed upon the DNA solution droplet and left for varying amounts of time at 23 °C (in most experiments, except where temperature was varied). Surface tension forces kept the disk on the droplet surface so that only the DNA uptake face of the PPy disk contacted the radiolabeled DNA solution. The substrate was subsequently washed in 1X TE buffer for 20 min. Anywhere from 6 to 12 droplets were made from the same DNA stock solution for a given experiment. When multiple droplets of the same concentration were used, larger droplets were made first and thoroughly mixed before aliquoting out 200 μL size droplets. Experiments in which only one experimental condition was varied were performed concurrently. This minimized any change in the stability of the DNA droplet or PPy substrate.

For experiments where the buffer and pH effects on DNA binding to PPy were examined, the EDTA content was decreased to 0.1 mM. When the buffer concentration was studied, TE buffer was prepared at Tris concentrations of 1 mM, 10 mM, 100 mM, and 1 M. Sodium phosphate buffer (Aldrich) was used for its greater buffering capacity. The ratio of mono- to dibasic phosphate was varied to make a final buffer concentration of 10 mM at pHs of 5.7, 7.15, and 8.2.

To denature the radiolabeled bacteriophage $\phi X174$ DNA, this was boiled in a tightly sealed polypropylene Eppendorf centrifuge tube for 30 min directly before incorporation into the final solution droplet.

Studies in Figure 6 involving desorption competition by calf thymus DNA were performed by first exposing PPy substrates to radiolabeled DNA droplets for 10 min followed by a brief wash in buffer and then exposure to competitor droplets for 10, 100, 200, and 1200 min. The competitor droplets contained either calf thymus DNA or 1X TE buffer. For the ^{32}P DNA uptake on presaturated PPy surface competition experiments, the PPy substrates were placed on top of droplets of solutions containing either calf thymus DNA, denatured calf thymus DNA, poly(styrenesulfonate) (PSS^-) (Polysciences, Inc.), 1X TE buffer, or TE buffer containing 0.5 mM phosphate buffer. The sodium salt of 99+% sulfonated poly(styrenesulfonate) was made from a narrow molecular weight distribution polystyrene with an average molecular weight of 5×10^5 g/mol. The concentration of the calf thymus DNA competitor varied depending on the experiment. In all cases, phenol-extracted calf thymus DNA (Sigma Chemical Co.) was used after cleavage by *Eco*RI and *Hind*III to give restriction fragments with an average length of 1100 bp.

Radioactivity from the ^{32}P-labeled DNA was detected using a high-voltage gas flow proportional counter. Radiation was detected in the β-ray plateau region at 1980 V using a Tennelec high-voltage power supply. The anodic detector chamber was purged at a constant rate of 60 cm^3/min with an argon gas mixture containing 10% methane. The detector had approximately a 40% efficiency for ^{32}P using isotope standards. All of the raw sample counts were corrected for control PPy disk background radioactivity (ca. 40 cpm), half-life decay, and detector efficiency and then coverted to ng of DNA per cm^2 surface area using the measured DNA batch specific activity.

While the DNA binding mass level was normalized to the apparent disk area for convenience in discussing the results, the real surface area of the PPy disks can vary. PPy synthesized in acetonitrile shows a less porous structure than that observed for PPy electropolymerized in water.[25] The solution face of electropolymerized PPy often grows with nodular, cauliflower-like surface features, which can contribute to additional surface area.[26] However, in this study, we did not address the issue of attempting to experimentally determine the real surface area of the disks. In more recent experiments to be reported elsewhere we address the question of PPy surface structure. These experiments are alluded to in our discussion of the results.

Shortening of the DNA chain length by ^{32}P radiodecay can be a problem in samples stored for extended time periods at high specific activities.[27] We documented this by gel electrophoresis (data not shown) in our ^{32}P DNA radiolabeling system. Based upon these data, radiolabeled DNA was only used in these experiments within 1 half-life (roughly 2 weeks) to avoid a significant chain shortening problem.

We have included error bars and values on only Figures 1 and 6 and Tables 1 and 2. In the case of the other figures and one table, error bars were not included since they are smaller than the point symbol itself. Error bars for individual points in most of the figures were calculated simply from the error inherent in the counting statistics ($(cpm)^{1/2}$) of that count level (cpm). This is because these points are the average of only duplicate values of the same experiment for which calculation of the standard error is meaningless. For Figures 1 and 6 and Table 1 we have given error bars and values as the standard error in the mean

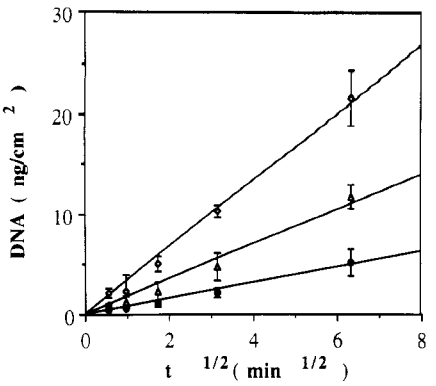

Figure 1. DNA adsorption onto PPy in 1X TE buffer, pH 8, at concentrations of (◇) 0.4, (△) 0.2, and (●) 0.1 μg/mL of DNA at 23 °C.

value because these experiments were repeated a statistically significant number of times.

Results and Discussion

DNA–Polypyrrole Binding Kinetics. The rate of DNA adsorption, dn/dt, onto a unit area of surface, in the absence of any sizable activation energy of surface binding, can be taken as

$$\frac{dn}{dt} = C_b\left(\frac{D}{\pi t}\right)^{1/2} \quad (1)$$

The rate of adsorption, or the mass of DNA molecules, n, per unit area, diffusing to the surface over a time, t, is proportional to the bulk solution concentration, C_b, the square root of the diffusion coefficient, D, and the inverse square root of time.[23,24]

Integration of eq 1 shows that the total mass of molecules, n, per unit area that have adsorbed to the surface at an elapsed time, t, is proportional to the square root of both t and D,

$$n = 2C_b\left(\frac{Dt}{\pi}\right)^{1/2} \quad (2)$$

We measured the uptake of DNA by PPy at 23 °C shown in Figure 1 for the three DNA concentrations, 0.1, 0.2, and 0.4 μg/mL. DNA uptake in ng/cm² is plotted against $t^{1/2}$. Two features are immediately apparent from this binding isotherm. First, it is clear that the initial rate of DNA adsorption onto PPy follows a $t^{1/2}$ dependence. Also, a trend toward greater adsorption of DNA by PPy with increasing DNA solution concentration is evident.

The $t^{1/2}$-dependent kinetic behavior was determined from the best fit log t exponent (0.49–0.50 for all data sets examined). The goodness of fit was determined by correlation to the t-distribution. The data fit well using the t-test performed at 95% confidence. It was concluded that DNA binding to PPy substrates follows $t^{1/2}$ kinetics in 1X TE buffer at concentrations of 0.1, 0.2, and 0.4 μg/mL of DNA at 23 °C. The linearity of this relation agrees with the diffusion-limited adsorption model.[23,24,28]

The calculated rate of adsorption increased linearly with DNA concentration. This is shown in Table 1, which compares the slopes of the binding isotherms and their normalized values at the three respective DNA concentrations. The trend and agreement with the equation (2) C_b dependence are expressed more clearly by the normalized rate of binding. Therefore, these results support the idea that the uptake follows classical diffusion-limited adsorption.

The diffusion coefficient, D, can be calculated by applying eq 2. The mean of a diffusion coefficient calculated from 15 separate uptake experiments was calculated to be 5.2×10^{-7} cm²/s. This may be compared to that measured for a DNA of 150 bp size, 2.6×10^{-7} cm²/s.[29] Given that the initial average molecular weight of the DNA polymer used in our experiment was 300 bp, it was thought at first that the diffusion coefficient should have been slightly smaller than that determined for the 150 bp DNA—not larger.

We suggest two possible reasons for this apparent discrepancy. Some of the apparent discrepancy in the diffusion coefficient value could be explained by a small decrease in the DNA molecular weight caused by the ^{32}P decay.[27] The second and more likely reason is that we are measuring the binding of a restriction fragment distribution of 18 different DNA sizes in these experiments. Since the shortest DNA fragments of the 18 total DNA size fragments (four shortest are 93, 84, 54, and 35 bp) have the largest diffusion coefficients, we may be measuring largely the diffusion of those fragments preferentially to the polypyrrole surface. This could easily account for the higher than expected diffusion coefficient calculated from the binding data in the complete absence of a radiolabeled fragment shortening effect.

Table 1. Calculated DNA Adsorption Compared As the Slopes of the Binding Isotherms

concn (C) (μg/mL)	slope[a] (ng/cm²·min$^{1/2}$)	normalized slope[b]
0.10	0.78 ● 0.14	1.0 ± 0.18
0.20	1.74 ± 0.21	2.2 ± 0.26
0.40	3.33 ● 0.31	4.3 ● 0.40

[a] Errors represent ± standard error of the mean. [b] Slope at C/slope at C = 0.1.

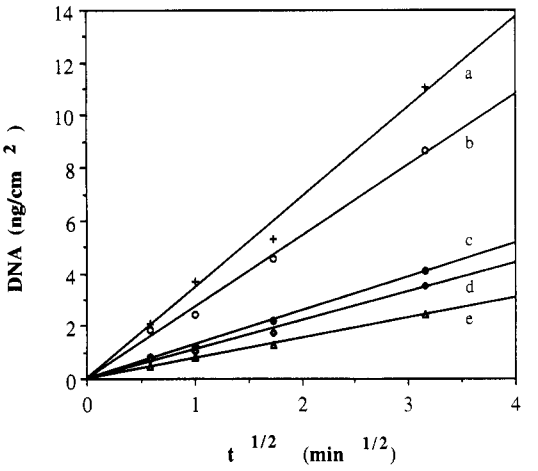

Figure 2. DNA adsorption onto PPy at five temperatures; (a) (+) 60 °C; (b) (○) 44 °C; (c) (●) 22 °C; (d) (◇) 7 °C; (e) (△) 3 °C. Binding of 0.2 μg/mL of DNA in 1X TE buffer, pH 8.

Activation Energy. We next asked the question whether the apparent diffusion-limited binding kinetics was accompanied by any significant energy barrier to binding in order to justify the applicability of this model. The apparent phenomenological activation energy, E_a, of the entire diffusion and binding process was determined from a study of the temperature-dependent initial binding kinetics using the Arrhenius relation. The results are presented in Figure 2 for five temperatures, 3, 7, 22, 44, and 60 °C, under our standard experimental conditions.

The plot for each temperature followed the characteristic $t^{1/2}$ kinetics of DNA uptake. As expected, an increase in the binding rate was observed on increasing the kinetic energy of the DNA molecules. The rate constant, k, was taken from the initial binding region at time t = 1 min. At 1 min, k is equivalent to the slope of the DNA adsorption

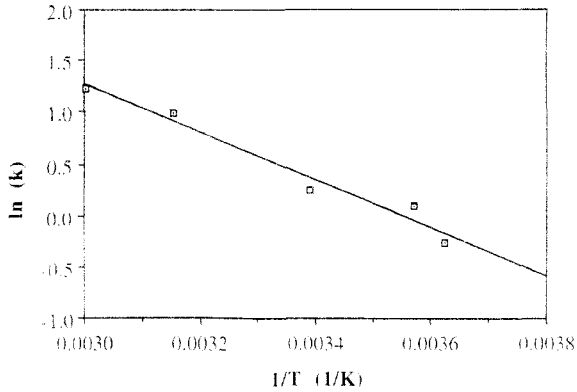

Figure 3. Arrhenius plot of the DNA adsorption data of the five temperatures in Figure 2. Each rate value, k, is expressed in ng/cm^2·min and was taken as dn/dt at $t^{1/2} = t = 1$ min from the Figure 2 data.

isotherm. An Arrhenius plot is presented in Figure 3. The activation energy, E_a, determined from the slope of the Arrhenius plot was 4.6 kcal/mol. This phenomenological activation energy barrier is the result of many processes including diffusion activation energy, activation energy of structural rearrangements prior to adsorption, and finally the adsorption activation energy which includes exchange of the tosylate counterion from the PPy positive charge group coordinated with the DNA phosphate binding. The low value of 4.6 kcal/mol suggests that none of the individual processes possesses any significant activation energy. This fact agrees with the diffusion-limited kinetic binding behavior measured for the DNA and also strongly suggests that the DNA binds in a native unaltered conformation since significant activation energy is required to interconvert DNA from the standard B structure to other secondary structures or to denature it.

Since the pH of Tris buffers is known to drop significantly with increasing temperature (−0.028 pH unit/°C), we determined that the magnitude of this effect on our determination of the E_a was at most 0.5 kcal/mol based upon the pH dependence of the DNA adsorption rate that we present later in this report. This yields at most a corrected E_a of 5.1 ± 0.5 kcal/mol, which leads to the same interpretation as above.

Ionic Concentration Effects. We next investigated the effect of solute ionic concentration on the rate of DNA binding. Since Tris buffer contains an ionic form (the monoacidic base: Tris-HCl), we varied the solution buffer concentration between 0.010 and 1 M. This effectively varied both the monovalent positive and negative ion concentrations between 0.00375 and 0.375 M. For this set of experiments, the EDTA concentration was reduced to 0.1 mM. Figure 4 demonstrates the buffer concentration effect on DNA binding rate. There was almost no measured difference in the binding rate for the 10 mM to 1 M buffer concentration range. This is in agreement with studies of ionic polyelectrolytes adsorbed onto oppositely charged surfaces, where the adsorption has been shown to be relatively concentration independent.[22] In contrast, equilibrium constants of DNA binding to proteins typically show that salt can have a great influence on binding affinity.[29-32]

Buffer Type and Solution pH. Since the studies presented to this point involved only Tris buffer at a single pH, it was of interest to find out whether the binding was affected by the buffer type or different pH values. To investigate both of these features, we chose 10 mM sodium phosphate buffers composed of a mixture of phosphate mono- and dibasic containing 0.1 mM EDTA at 23 °C.

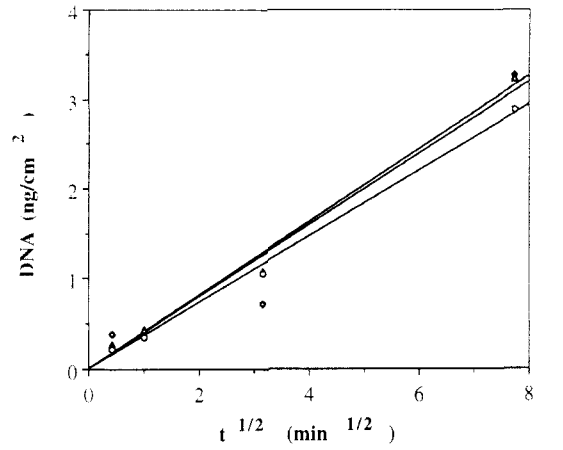

Figure 4. DNA binding at ionic concentrations of (●) 10 mM, (△) 100 mM, and (◇) 1 M Tris buffer, pH 8, at 23 °C and 0.2 μg/mL of DNA.

Table 2. Comparison of the Binding Rates Obtained from the Slope of Binding of DNA to PPy

buffer	sol pH	binding rate (ng/cm^2·min)
Tris	7.8	1.58 ± 0.16
phosphate	7.8	1.48 ± 0.014
phosphate	5.7	1.28 ± 0.008
phosphate	7.15	1.56 ± 0.01
phosphate	8.2	1.35 ± 0.01

The effect of the buffer type was studied by comparing Tris and phosphate buffers at pH 7.8 and otherwise standard processing conditions. In the experiment comparing the solution pH, the final pH values of the phosphate buffers were 5.7, 7.15, and 8.2.

The binding kinetics were relatively unaffected by pH and buffer changes. Adherence to $t^{1/2}$ kinetics was maintained with minor changes in the rate of DNA uptake. These data are tabulated in Table 2. It can be seen that a buffer change from Tris to phosphate does not significantly affect the binding rate under the standard experimental conditions. The DNA adsorption rates for the four pH values demonstrated a pH maximum close to 7, with a drop off in binding rate of at most 20% in the pH range 5.0–8.5. A similar effect was observed for DNA binding to negatively charged sand, which showed a binding maximum at pH 7.0.[19] In basis pH solutions, increasing hydroxide ion concentration or, more importantly, the increasing concentration of doubly negatively charged phosphate ion species may compete more effectively with DNA for binding sites on the positively charged PPy surface, lowering the adsorption rate as we observe here.

Native vs Single-Stranded DNA Binding. We next investigated whether the binding of single-stranded *φX174* DNA fragments differs significantly from the binding of double-stranded fragments. In Figure 5 we compare the binding of the single-stranded form (denatured by boiling and quick cooled) to the native, double-helical form of DNA under the standard experimental conditions. The slope of the binding for the single-stranded DNA was greater than the slope of binding of the double-helical DNA, although the error levels were significant. The increased binding rate of the single-stranded form could be attributed to either differences in DNA solution dynamic properties or binding site availability in the two forms or both. For example, double-helical DNA of a few hundred base pairs is a relatively rigid rodlike molecule[33] while single stranded DNA of any size is a relatively flexible, very much compacted structure which possesses small regions of double helix along with disordered regions

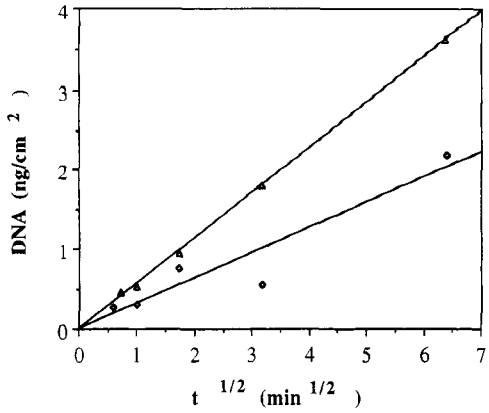

Figure 5. Compared adsorption of heat-denatured (△) single-stranded DNA to the adsorption of (◇) double-stranded DNA in 1X TE buffer, pH 8, at 23 °C.

in which the bases themselves would be available to interact with the polypyrrole chain.

Considerations of structural differences aside, the more rapid diffusion of single-stranded DNA may be explained purely on the basis of diffusion coefficient differences. Although the Kirkwood–Riseman theory was developed for linear, flexible-chain polymers, it can provide a qualitative understanding of the difference in the diffusion properties between flexible and rigid rod polymers.[34] The theory demonstrates that the diffusion coefficient is inversely proportional to both the molecular weight of the macromolecule and the root mean square end-to-end distance of the coiled chain. As the DNA is "melted", both the molecular weight and the end-to-end distance are decreased. Based on these two factors, it would be expected that the diffusion coefficient and likewise the adsorption rate would be greater for the single-stranded DNA.

Desorption, Competition, and Reversibility of Binding. Our results to date suggest that DNA binds to polypyrrole without significant alteration of its structure. Our working hypothesis has been that DNA is reversibly bound to the PPy surface. We next determined to test this idea directly. Being a macromolecule, DNA possesses a large number of binding sites at which multiple interactions with the PPy surface are likely to occur simultaneously. Because of multiple binding sites, most polymer adsorptions are considered as practically irreversible.[22] In the experiments that follow, we first investigated the reversibility of binding by a desorption kinetic study. This was followed by an experiment in which we measured the uptake of radiolabled DNA by PPy surfaces that had been first exposed to and saturated by competitor molecules.

In the desorption experiment, DNA was initially adsorbed identically onto a series of PPy disks for 1 h at a concentration of 0.2 μg/mL of DNA in 1X TE buffer at 23 °C. Immediately, each disk was quickly rinsed to remove unadsorbed DNA. The subsequent desorption kinetics of DNA from each of the disks into a droplet of 1X TE buffer in the presence and absence of an excess of unlabeled calf thymus DNA were determined and are displayed in Figure 6. The rate of desorption in the absence of calf thymus DNA is reasonably fit by a single-exponential curve. The data yield an initial calculated value of ca. 0.006 ng/cm²·min DNA loss. This is about 2 orders of magnitude slower than the rate of uptake. The slow desorption rate led to the choice of a standard 20-min wash time in the protocol of all DNA binding experiments discussed previously, since the loss of material is rather insignificant at this time.

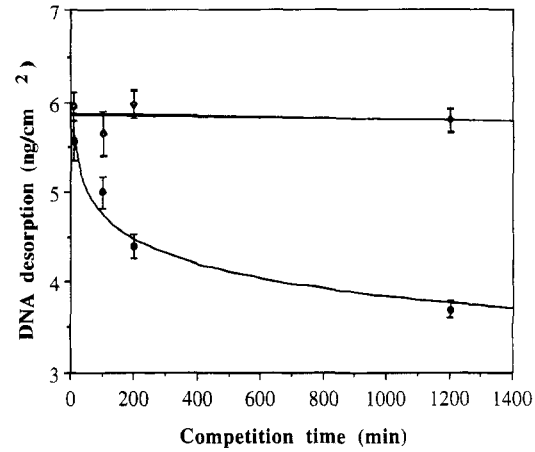

Figure 6. Desorption of ^{32}P-labeled DNA in the presence of (◇) 43 μg/mL competitor calf thymus DNA and (●) 1X TE buffer alone. For the sake of comparison, the calf thymus DNA curve is shown by a linear fit and the TE buffer curve is shown to fit a logarithmic desorption.

The fast initial desorption rate may be due to DNA residing in internal channels of the polypyrrole disks. We have recently obtained evidence for channel structures using scanning electron microscopy and high-resolution transmission electron microscopy of the disk surfaces as well as the interior. In support of this possibility, there is a measurable migration of radiolabeled DNA through the disk interior during the course of DNA uptake.[35] The lack of significant desorption of labeled DNA from internal channels in the presence of a high concentration of unlabeled DNA may be due to an unfavorable chemical potential preventing DNA diffusion back into the droplet. Alternatively, there may be a physical blockage of absorbed DNA in internal channels or entanglement of bound DNA with unlabeled competitor DNA.

The desorption rate that is observed at longer times was very slow. As is the case for certain polymeric systems,[24] this slow desorption may reflect the fact that DNA is bound to the PPy surface at multiple binding sites.

^{32}P DNA Uptake on Presaturated PPy Surfaces. These experiments investigated the uptake of ^{32}P DNA onto PPy disks that had been presaturated by other molecules. Results from these experiments rank the ability of the ^{32}P radiolabeled DNA molecules to bind to unoccupied sites or displace other molecules bound to the PPy surface. For presaturation, the PPy substrates were placed on droplets containing calf thymus DNA, denatured calf thymus DNA, poly(styrenesulfonate) (PSS^-), TE buffer, or TE buffer containing phosphate buffer for 2 days at ice bath temperature. All of the solutions contained 1X TE buffer. Following this presaturation step, each substrate was quickly rinsed in 1X TE buffer and placed on standard droplets of ^{32}P-labeled *φX174* DNA for various times. The overall results of these binding studies are displayed in Figure 7. By comparing the best fit slopes of these binding kinetics, the calculated adsorption rates can be compared in Table 3.

It is clear that *φX174* DNA adsorbs onto PPy substrates presaturated with phosphate containing 1X TE buffer far more easily than any of the polyanions. Except for the phosphate containing 1X TE buffer solution, the data given in Figure 7 are noisy but all polyanions demonstrate reasonable fits to the $t^{1/2}$ functional dependence. There is a clear trend to the comparative ^{32}P-labeled DNA uptake rates, from the highest to lowest in the following order of presaturation species: single-stranded DNA > PSS^- > double-helical DNA.

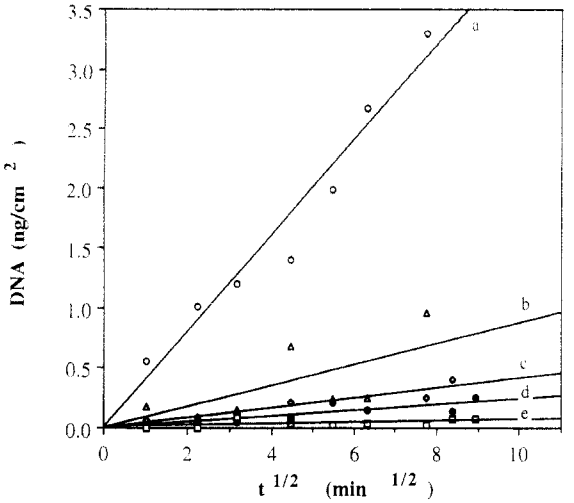

Figure 7. Standard adsorption of ^{32}P-labeled *φX174* DNA onto PPy presaturated for 2 days with phosphate containing (a) (○) 1X TE buffer, (b) (△) 57 μg/mL single-stranded calf thymus DNA, (c) (◇) 30 μg/mL PSS$^-$, and double-helical calf thymus DNA at concentrations of (d) (●) 17 and (e) (□) 57 μg/mL.

Table 3. Relative ^{32}P DNA Uptake by Presaturated PPy Surfaces

polymer presatd on PPy	polymer concn (μg/mL)	rel DNA uptake[a] (ng/cm)^2/min
1X TE buffer		1.00 (0.40)
single-stranded DNA	57	0.22 (0.087)
poly(styrenesulfonate)	30	0.11 (0.041)
calf thymus DNA	17	0.06 (0.024)
calf thymus DNA	57	0.02 (0.0071)

[a] Actual uptake rate values are presented in parentheses while relative values are based on the 1X TE buffer presaturated surface being unity.

The most effective presaturation condition was the higher concentration double-helical DNA. PPy disks bound the labeled DNA about 50 times slower when presaturated with 57 μg/mL calf thymus DNA compared to presaturation in phosphate, 1X TE buffer. The next most effective surface presaturation condition was the 17 μg/mL calf thymus DNA to which labeled DNA bound 16 times slower than to the buffer-presaturated surface. It is understandable that the ^{32}P-labeled DNA would bind less rapidly to a PPy substrate presaturated in the higher 57 μg/mL calf thymus double-helical DNA than in the lower 17 μg/mL concentration. With more DNA in solution, it is expected that a more complete saturation of the binding sites would be achieved.

There was a 5-fold higher ^{32}P DNA binding rate to PPy presaturated with PSS$^-$ in comparison to the higher calf thymus DNA presaturation condition. This experiment was designed to have 57 μg/mL calf thymus DNA as the presaturation solution, equivalent in total negative charge groups to 30 μg/mL PSS$^-$. Why was the double-helical DNA so superior in presaturation? While other arguments could probably be offered for differences in equilibrium presaturation strengths, we feel the most likely explanation lies in the extremely high electrostatic potential that has been calculated to lie in the immediate environment of the double-helical DNA groove structure.[36] This electrostatic potential is significantly greater than that for single-stranded DNA and may be greater than the PSS$^-$ potential. Therefore, it should be more effective at attracting positive charge density on the PPy polymer chain, creating a stronger interaction, consequently being harder to displace that the other presaturation polymers. Accordingly, we find single-stranded DNA at equivalent charge concentration to be around 10-fold poorer than double-helical DNA at presaturating the surface to prevent radiolabeled DNA binding. Fitting in with this convenient explanation, PSS$^-$ is 2-fold better at presaturating the PPy surface compared to single-stranded DNA. To a first approximation, PSS$^-$ ought to have a higher negative charge density and therefore a higher electrostatic potential along the chain compared to single-stranded DNA because its monomer unit mass is considerably lower than the 330 g/mol of single-stranded DNA.

Differences in the stereochemistry of the phosphate and sulfonate ion binding to the positively charged functional groups on the PPy surface may also have a significant effect on the differences measured. For example, substantial anion dopant effects on electrochemically prepared oxidized PPy thin film properties such as conductivity have been observed.[37] Other differences in the noncovalent interactions of the monomer units presented by all three presaturation polyanions may also have a marked effect on their ability to influence subsequent adsorption rates by labeled DNA.

Conclusions

The rate of solution adsorption of DNA to a polypyrrole substrate surface occurred with a $t^{1/2}$ dependence and was linear in DNA concentration. The data were shown to obey the Arrhenius relation, giving a low activation energy of about 5 kcal/mol. These results are in agreement with diffusion-limited adsorption with no significant activation energy barrier to binding. The data also suggest that the DNA binds to PPy without significant alteration of its structure. There is little difference in DNA binding rate in the 0.004–0.375 M counterion concentration range. The binding was relatively unaffected by substitution of the TE buffer with phosphate buffer. A minor pH dependence to the binding rate with maximum close to 7 was determined. The single-stranded form of *φX174* DNA bound to the PPy surface with faster $t^{1/2}$ kinetics than the double-stranded form. In related studies we have shown that binding of double-helical DNA to PPy is absolutely dependent upon the presence of the electrooxidized positively charged surface functional groups.[38] The very high electrostatic potential in the grooves of the double helix can explain its very high affinity for the charged PPy surface and its effectiveness in the presaturation competition experiments.

In summary, polypyrrole and other conducting polymers[35,38–40] appear to be promising substrates for the reversible binding of DNA and other polyanions. Their novel electronic and optical properties provide intriguing possibilities for use in biosensor and biotechnological device applications. In conjunction with their rational structural modification, incorporation of biological macromolecules such as DNA into novel molecular architectures possessing intelligent properties may be useful for device applications.

Acknowledgment. We acknowledge support from ARO Grant DAAL03-91-G-0064.

References and Notes

(1) Diaz, A. F.; Bargon, J. Electrochemical Synthesis of Conducting Polymers. In *Handbook of Conducting Polymers*; Skotheim, T. A., Ed.; Marcel Dekker: New York, 1986; Vol. 1, p 81.

(2) Jasne, S. Polypyrroles. In *Encyclopedia of Polymer Science and Engineering*; Mark, H. F., Bikales, N. M., Overberger, C. G., Mengies, G., Eds.; John Wiley and Sons: New York, 1986; Vol. 13, p 42.

(3) Moss, B. K.; Burford, R. P.; Skyllas-Kazacos, M. *Mater. Forum* **1989**, *13*, 35.
(4) Satoh, M.; Kaneto, K.; Yoshino, K. *Synth. Met.* **1986**, *14*, 289.
(5) Diaz, A. F.; Hall, B. *IBM J. Res. Dev.* **1983**, *27*, 342.
(6) Waller, A. M.; Compton, R. G. *J. Chem. Soc., Faraday Trans. 1* **1989**, *85* (4), 977.
(7) Devreux, F.; Genoud, F.; Nechtschein, M.; Villeret, B. *Synth. Met.* **1987**, *18*, 89.
(8) Dong, S.; Ding, J.; Zhan, R. *J. Chem. Soc., Faraday Trans. 1* **1989**, *85* (7), 1599.
(9) Wynne, K. J.; Street, G. B. *Macromolecules* **1985**, *18*, 2361.
(10) Zinger, B.; Miller, L. L. *J. Am. Chem. Soc.* **1984**, *106*, 6861.
(11) Miller, L. L.; Zhou, Q. N. *Macromolecules* **1987**, *20*, 1594.
(12) Boyle, A.; Genies, E.; Fouletier, M. *J. Electroanal. Chem.* **1990**, *279*, 179.
(13) Folds, N. C.; Lowe, C. R. *J. Chem. Soc., Faraday Trans. 1* **1986**, *82*, 1265.
(14) Smith, A. B.; Knowles, C. J. *Biotechnol. Appl. Biochem.* **1990**, *12*, 661.
(15) Wnek, G. E.; Prezyna, L. A.; Lee, J. J.; Qiu, Y.-J.; Reynolds, J. R. *Polym. Prepr. (Am. Chem. Soc., Div. Polym. Chem.)* **1989**, *30* (2), 178.
(16) Wolf, S. F.; Haines, L.; Fisch, J.; Kremsky, J. N.; Dougherty, J. P.; Jacobs, K. *Nucleic Acids Res.* **1987**, *15*, 2911.
(17) Kawaguchi, H.; Asai, A.; Ohtsuka, Y.; Watanabe, H.; Wada, T.; Handa, H. *Nucleic Acids Res.* **1989**, *17*, 6229.
(18) Clore, G. M.; Gronenborn, A. M.; Davis, R. W. *J. Mol. Biol.* **1982**, *155*, 447.
(19) Lorenz, M. G.; Wackernagel, W. *Appl. Environ. Microbiol.* **1987**, *53*, 2948.
(20) Davidson, J. N. In *The Biochemistry of the Nucleic Acids*, 7th ed.; Chapman and Hall and Science Paperbacks: Norfolk, Great Britain, 1972; p 148.
(21) Guschlbauer, W.; Saenger, W. *DNA–Ligand Interactions From Drugs to Proteins*; Plenum Press: New York, 1987.
(22) Hesselink, F. TH. Adsorption of Polyelectrolytes From Dilute Solution. In *Adsorption from Solution at the Solid/Liquid Interface*; Parfitt, G. D., Rochester, C. H., Eds.; Academic Press: London, 1983; p 377.
(23) Davies, J. T.; Rideal, E. K. In *Interfacial Phenomena*; Academic Press: New York, 1961; p 154.
(24) Andrade, J. D.; Hlady, V. *Adv. Polym. Sci.* **1986**, *79*, 1.
(25) Ko, J. M.; Rhee, H. W.; Park, S.-M.; Kim, C. Y. *J. Electrochem. Soc.* **1990**, *137*, 905.
(26) Cvetko, B. F.; Brungs, M. P.; Burford, R. P.; Skyllas-Kazacos, M. *J. Mater. Sci.* **1988**, *23*, 2102.
(27) Hodgson, C. P.; Fisk, R. Z.; Willit, L. B. *Biotechniques* **1988**, *6* (3), 208.
(28) Tyn, M. T.; Gusek, T. W. *Biotechnol. Bioeng.* **1990**, *35*, 327.
(29) Nicolai, T.; Mandel, M. *Macromolecules* **1989**, *22*, 2348.
(30) Sunderman, F. W.; Barber, A. M. *Ann. Clin. Lab. Sci.* **1988**, *18*, 267.
(31) Petri, I.; Weller, K.; Zinke, M. *Bioelectrochem. Bioenerget.* **1988**, *19*, 95.
(32) Record, M. T.; Mazur, S. J.; Melancon, P.; Roe, J.-H.; Shoner, S. L.; Unger, L. In *Annu. Rev. Biochem.* **1981**; *50*, 997.
(33) Hogan, M.; Wang, J.; Austin, R. H.; Monitto, C. L.; Hershkowitz, S. *Proc. Natl. Acad. Sci. U.S.A.* **1982**, *79*, 3518.
(34) Vrentas, J. S.; Duda, J. L. In *Encyclopedia of Polymer Science and Engineering*; Mark, H. F., Bikales, N. M., Overberger, C. G., Mengies, G., Eds.; John Wiley and Sons: New York, 1986; Vol. 5, p 46.
(35) Pande, R.; Lim, J. O.; Marx, K. A.; Tripathy, S. K.; Kaplan, D. L. In *Biomolecular Materials*; Materials Research Society: Pittsburgh, 1993; Vol. 292, p 135.
(36) Pullman, B.; Lavery, R.; Pullman, A. *Eur. J. Biochem.* **1982**, *124*, 229.
(37) *Handbook of Conducting Polymers*; Skotheim, T. A., Ed.; Marcel Dekker: New York, 1986.
(38) Minehan, D. S.; Marx, K. A.; Tripathy, S. K. *Proc. Am. Chem. Soc. Div. Polym. Mater.: Sci. Eng.* **1991**, *64*, 341.
(39) Lim, J. O.; Minehan, D. S.; Marx, K. A.; Tripathy, S. K. In *Hierarchically Structured Materials*; Materials Research Society: Pittsburgh, 1993; Vol. 255, p 195.
(40) Marx, K. A.; Minehan, D. S.; Lin, J. O.; Kamath, M.; Tripathy, S.; Kaplan, D. L. In *Proceedings of the First International Conference on Intelligent Materials*; Technomic: Japan, 1992; p 78.